Perturbatively improving RI-MOM renormalization constants

M. Constantinou[1], M. Costa[1], M. Göckeler[2], R. Horsley[3],
H. Panagopoulos[1], H. Perlt[4], P. E. L. Rakow[5], G. Schierholz[6] and
A. Schiller[4]

[1] *Department of Physics, University of Cyprus, P.O.Box 20537, Nicosia CY-1678, Cyprus*
[2] *Institut für Theoretische Physik, Universität Regensburg, 93040 Regensburg, Germany*
[3] *School of Physics, University of Edinburgh, Edinburgh EH9 3JZ, UK*
[4] *Institut für Theoretische Physik, Universität Leipzig, 04103 Leipzig, Germany*
[5] *Theoretical Physics Division, Department of Mathematical Sciences,
University of Liverpool, Liverpool L69 3BX, UK*
[6] *Deutsches Elektronen-Synchrotron DESY, 22603 Hamburg, Germany*

Abstract

The determination of renormalization factors is of crucial importance in lattice QCD. They relate the observables obtained on the lattice to their measured counterparts in the continuum in a suitable renormalization scheme. Therefore, they have to be computed as precisely as possible. A widely used approach is the nonperturbative Rome-Southampton method. It requires, however, a careful treatment of lattice artifacts. In this paper we investigate a method to suppress these artifacts by subtracting one-loop contributions to renormalization factors calculated in lattice perturbation theory. We compare results obtained from a complete one-loop subtraction with those calculated for a subtraction of contributions proportional to the square of the lattice spacing.

1   Introduction

Renormalization factors in lattice Quantum Chromodynamics (QCD) relate observables computed on finite lattices to their continuum counterparts in specific renormalization schemes. Therefore, their determination should be as precise as possible in order to allow for a reliable comparison with experimental results. One approach is based on lattice perturbation theory [1]. However, it suffers from its intrinsic complexity, slow convergence and the impossibility to handle mixing with lower-dimensional operators. Therefore, nonperturbative methods have been developed and applied. Among them the so-called Rome-Southampton method [2] (utilizing the RI-MOM scheme) is widely used because of its simple implementation. It requires, however, gauge fixing.

Like (almost) all quantities evaluated in lattice QCD also renormalization factors suffer from discretization effects. One can attempt to cope with these lattice artifacts by extrapolating the nonperturbative scale dependence to the continuum (see Ref. [3]) or one can

try to suppress them by a subtraction procedure based on perturbation theory. Here we shall deal with the latter approach.

In a recent paper of the QCDSF/UKQCD collaboration [4] a comprehensive discussion and comparison of perturbative and nonperturbative renormalization have been given. Particular emphasis was placed on the perturbative subtraction of the unavoidable lattice artifacts. For simple operators this can be done in one-loop order completely by computing the corresponding diagrams for finite lattice spacing numerically. While being very effective this procedure is rather involved and not suited as a general method for more complex operators, especially for operators with more than one covariant derivative, and complicated lattice actions. An alternative approach can be based on the subtraction of one-loop terms of order a^2 with a being the lattice spacing. The computation of those terms has been developed by the authors of Ref. [6] and applied to various operators for different actions. In this paper we use some of those results for the analysis of Monte Carlo data for renormalization coefficients.

We study the flavor-nonsinglet quark-antiquark operators given in Table 1. The cor-

Operator (multiplet)	Notation	Representation	Operator basis
$\bar{u}\,d$	$\mathcal{O}^S$	$\tau_1^{(1)}$	$\mathcal{O}^S$
$\bar{u}\,\gamma_\mu\,d$	$\mathcal{O}^V_\mu$	$\tau_1^{(4)}$	$\mathcal{O}^V_1, \mathcal{O}^V_2, \mathcal{O}^V_3, \mathcal{O}^V_4$
$\bar{u}\,\gamma_\mu\gamma_5\,d$	$\mathcal{O}^A_\mu$	$\tau_4^{(4)}$	$\mathcal{O}^A_1, \mathcal{O}^A_2, \mathcal{O}^A_3, \mathcal{O}^A_4$
$\bar{u}\,\sigma_{\mu\nu}\,d$	$\mathcal{O}^T_{\mu\nu}$	$\tau_1^{(6)}$	$\mathcal{O}^T_{12}, \mathcal{O}^T_{13}, \mathcal{O}^T_{14}, \mathcal{O}^T_{23}, \mathcal{O}^T_{24}, \mathcal{O}^T_{34}$
$\bar{u}\,\gamma_\mu\,\overset{\leftrightarrow}{D}_\nu\,d$	$\mathcal{O}_{\mu\nu} \to \mathcal{O}^{v2,a}$	$\tau_3^{(6)}$	$\mathcal{O}_{\{12\}}, \mathcal{O}_{\{13\}}, \mathcal{O}_{\{14\}}, \mathcal{O}_{\{23\}}, \mathcal{O}_{\{24\}}, \mathcal{O}_{\{34\}}$
$\bar{u}\,\gamma_\mu\,\overset{\leftrightarrow}{D}_\nu\,d$	$\mathcal{O}_{\mu\nu} \to \mathcal{O}^{v2,b}$	$\tau_1^{(3)}$	$1/2(\mathcal{O}_{11} + \mathcal{O}_{22} - \mathcal{O}_{33} - \mathcal{O}_{44}),$ $1/\sqrt{2}(\mathcal{O}_{33} - \mathcal{O}_{44}), 1/\sqrt{2}(\mathcal{O}_{11} - \mathcal{O}_{22})$

Table 1: Operators and their representations as investigated in the present paper. The symbol $\{...\}$ means total symmetrization. A detailed group theoretical discussion is given in [5].

responding renormalization factors have been measured (and chirally extrapolated) at $\beta = 5.20, 5.25, 5.29$ and 5.40 using $N_f = 2$ clover improved Wilson fermions with plaquette gauge action [4]. All results are computed in Landau gauge. The clover parameter c_{SW} used in the perturbative calculation discussed below is set to its lowest order value $c_{SW} = 1$.

2 Renormalization group invariant operators

We define the renormalization constant Z of an operator $\mathcal{O}$ from its amputated Green function (or vertex function) $\Gamma(p)$, where p is the external momentum and the operator is taken at vanishing momentum. The corresponding renormalized vertex function and the Born term (with all lattice artifacts included) are denoted by $\Gamma_R(p)$ and $\Gamma^{\text{Born}}(p)$,

respectively. If there is no mixing, Z can then be obtained by imposing the condition

$$\frac{1}{12} \, \mathrm{tr} \left[\Gamma_R(p) \, \Gamma^{\mathrm{Born}}(p)^{-1} \right] = 1 \tag{1}$$

for vanishing quark mass at $p^2 = \mu^2$, where μ is the renormalization scale. The Z factor relates the renormalized and the unrenormalized vertex function through

$$\Gamma_R(p) = Z_q^{-1} \, Z \, \Gamma(p) \,, \tag{2}$$

with Z_q being the quark field renormalization constant determined by

$$Z_q(p) = \frac{\mathrm{tr} \left[-\mathrm{i} \sum_\lambda \gamma_\lambda \sin(ap_\lambda) \, aS^{-1}(p) \right]}{12 \sum_\nu \sin^2(ap_\nu)} \tag{3}$$

in the chiral limit again at $p^2 = \mu^2$. Condition (1) together with (3) defines the RI$'$-MOM renormalization scheme. Here S^{-1} is the inverse quark propagator. Using (1) we compute Z from

$$Z_q^{-1} \, Z \, \frac{1}{12} \, \mathrm{tr} \left[\Gamma(p) \, \Gamma^{\mathrm{Born}}(p)^{-1} \right] = 1 \,. \tag{4}$$

For operators transforming as singlets under the hypercubic group $H(4)$, such as $\mathcal{O}^S$, Z can depend on the components of p only through $H(4)$ invariants.

For operators belonging to an $H(4)$ multiplet of dimension greater than 1 the condition (1) violates $H(4)$ covariance and would in general lead to different Z factors for each member of the multiplet. In Ref. [4] an averaging procedure has been proposed to calculate one common Z factor for every multiplet. Labeling the chosen operator basis by $i = 1, 2, \ldots, d$ the common Z was calculated from

$$Z_q^{-1} \, Z \, \frac{1}{d} \sum_{i=1}^d \frac{1}{12} \, \mathrm{tr} \left[\Gamma_i(p) \Gamma_i^{\mathrm{Born}}(p)^{-1} \right] = 1 \,. \tag{5}$$

This condition leads to an $H(4)$-invariant Z for the operators without derivatives in Table 1. However, in general this is not the case.

It is not difficult to devise a renormalization condition that respects the hypercubic symmetry. Choosing a basis of operators (again labeled by i), transforming according to a unitary irreducible representation of $H(4)$, the relation

$$Z_q^{-1} \, Z \, \frac{\sum_{i=1}^d \mathrm{tr} \left[\Gamma_i(p) \Gamma_i^{\mathrm{Born}}(p)^\dagger \right]}{\sum_{j=1}^d \mathrm{tr} \left[\Gamma_j^{\mathrm{Born}}(p) \Gamma_j^{\mathrm{Born}}(p)^\dagger \right]} = 1 \tag{6}$$

defines a Z factor which is invariant under $H(4)$, provided that the quark field renormalization factor is also $H(4)$ invariant. The derivation of renormalization condition (6) is given in the Appendix. For the operators without derivatives the definitions (6) and (5) are equivalent. For the considered operators with one derivative the resulting differences turn out to be negligible. In the following the Z factors will be determined from (6) using the operator bases given in Table 1. This is our version of the RI$'$-MOM scheme.

We define a so-called RGI (renormalization group invariant) operator, which is independent of scale M and scheme $\mathcal{S}$, by [4]

$$\mathcal{O}^{\mathrm{RGI}} = \Delta Z^{\mathcal{S}}(M)\, \mathcal{O}^{\mathcal{S}}(M) = Z^{\mathrm{RGI}}(a)\, \mathcal{O}_{\mathrm{bare}} \tag{7}$$

with

$$\Delta Z^{\mathcal{S}}(M) = \left(2\beta_0 \frac{g^{\mathcal{S}}(M)^2}{16\,\pi^2}\right)^{-(\gamma_0/2\beta_0)} \exp\left\{\int_0^{g^{\mathcal{S}}(M)} dg' \left(\frac{\gamma^{\mathcal{S}}(g')}{\beta^{\mathcal{S}}(g')} + \frac{\gamma_0}{\beta_0 g'}\right)\right\} \tag{8}$$

and the RGI renormalization constant (depending on a via the lattice coupling)

$$Z^{\mathrm{RGI}}(a) = \Delta Z^{\mathcal{S}}(M)\, Z^{\mathcal{S}}_{\mathrm{bare}}(M, a)\,. \tag{9}$$

Here $g^{\mathcal{S}}$, $\gamma^{\mathcal{S}}$ and $\beta^{\mathcal{S}}$ are the coupling constant, the anomalous dimension and the β-function in scheme $\mathcal{S}$, respectively. Relations (7), (8) and (9) allow us to compute the operator $\mathcal{O}$ in any scheme and at any scale we like, once Z^{RGI} is known. Therefore, the knowledge of Z^{RGI} is very useful for the renormalization procedure in general. Ideally, Z^{RGI} depends only on the bare lattice coupling, but not on the momentum p. Computed on a lattice, however, it suffers from lattice artifacts, e.g., it contains contributions proportional to $a^2 p^2$, $(a^2 p^2)^2$ etc. For a precise determination it is essential to have these discretization errors under control.

As the RI$'$-MOM scheme is in general not $O(4)$-covariant even in the continuum limit, it is not very suitable for computing the anomalous dimensions needed in (8). Therefore we use an intermediate scheme $\mathcal{S}$ with known anomalous dimensions and calculate Z^{RGI} as follows:

$$Z^{\mathrm{RGI}}(a) = \Delta Z^{\mathcal{S}}(M = \mu)\, Z^{\mathcal{S}}_{\mathrm{RI}'-\mathrm{MOM}}(M = \mu)\, Z^{\mathrm{RI}'-\mathrm{MOM}}_{\mathrm{bare}}(\mu, a)\,. \tag{10}$$

It turns out that a type of momentum subtraction scheme is a good choice for $\mathcal{S}$ (for details see Ref. [4]). The formula which is used to compute the transformation factor $Z^{\mathcal{S}}_{\mathrm{RI}'-\mathrm{MOM}}(\mu)$ is given there together with all needed coefficients of the β-function and anomalous dimensions, which are based on continuum three-loop calculations such as those in [7, 8, 9].

On a lattice with linear extent L the scale μ should ideally fulfill the relation

$$1/L^2 \ll \Lambda^2_{\mathrm{QCD}} \ll \mu^2 \ll 1/a^2\,. \tag{11}$$

In that case $Z^{\mathrm{RGI}}(a)$ would be independent of μ, and from the resulting plateau we could read off the corresponding final value. However, in practice $a\mu$ is not necessarily small leading to non-negligible lattice artifacts that have to be tamed. A promising tool to control lattice artifacts in a systematic way is lattice perturbation theory: We expect that after subtracting these perturbative terms the calculation of the Z factors can be done more accurately.

4

3 Subtraction of all lattice artifacts in one-loop order

In standard lattice perturbation theory the one-loop renormalization constants are given in the form

$$Z(\mu, a) = 1 + \frac{g^2 \, C_F}{16 \, \pi^2} \, (\gamma_0 \, \ln(a\mu) + \Delta), \quad C_F = \frac{4}{3}. \tag{12}$$

This means that the a-dependence is retained only in the logarithm and implicitly in g, while in all other contributions the limit $a \to 0$ has been taken.

However, there is no need to do so. We can keep a finite everywhere and thus evaluate the lattice artifacts at one-loop order completely, proceeding as follows. Let us denote by $F(p, a)$ the total one-loop correction and by $\tilde{F}(p, a)$ the expression resulting from $F(p, a)$ by neglecting all contributions which vanish for $a \to 0$. The difference

$$D(p, a) = F(p, a) - \tilde{F}(p, a) \tag{13}$$

represents the lattice artifacts in one-loop perturbation theory and is used to correct for the discretization errors:

$$Z_{\text{bare}}^{\text{RI}'-\text{MOM}}(p, a)_{\text{MC,sub}} = Z_{\text{bare}}^{\text{RI}'-\text{MOM}}(p, a)_{\text{MC}} - \frac{g_\star^2}{16 \, \pi^2} C_F \, D(p, a). \tag{14}$$

There is a certain freedom in choosing the coupling $g_\star$ in (14). It turned out that the use of the boosted coupling

$$g_{\text{B}}^2 = \frac{g^2}{P(g)} = g^2 + O(g^4) \tag{15}$$

($P(g)$ being the measured plaquette at $\beta = 6/g^2$) is quite successful in estimating the higher-order discretization effects. With the prescription (14) all lattice artifacts in one-loop order are subtracted.

In Fig. 1 we show the effect of subtraction on the RGI renormalization factors for selected operators of Table 1. For all operators we recognize after subtraction a remarkable smoothing and a pronounced plateau as a function of p^2 for $p^2 \gtrsim 10\,\text{GeV}^2$. The large bending in the small p^2 region might indicate the breakdown of perturbation theory (cf. the discussion in [4]). The examples show that the one-loop subtraction of lattice artifacts (14) works very well and, moreover, is needed for a precise determination of the renormalization constants. The final values for Z^{RGI} from (10) are obtained by a fit with an ansatz [4]

$$Z_{\text{RI}'-\text{MOM}}^{\mathcal{S}}(p) \, Z_{\text{bare}}^{\text{RI}'-\text{MOM}}(p, a)_{\text{MC,sub}} = \frac{Z^{\text{RGI}}(a)}{\Delta Z^{\mathcal{S}}(p) \, [1 + b_1 \, (g^{\mathcal{S}})^8]} + c_1 \, a^2 p^2. \tag{16}$$

The free parameter b_1 takes into account that the transformation factor $Z_{\text{RI}'-\text{MOM}}^{\mathcal{S}}(p)$ is known to three-loop order $(g^{\mathcal{S}})^6$ only. Further possible lattice artifacts are parametrized by $c_1 \, a^2 p^2$.

For practical reasons the numerical calculation of $F(p, a)$ - and therefore the calculation of Z^{RGI} using (16) - is restricted to operators with at most one derivative and for $N_f = 2$ only. In order to perform the subtraction for a wider class of operators and/or for $N_f = 2+1$ (where the considered lattice action becomes more complicated) we have to look for an
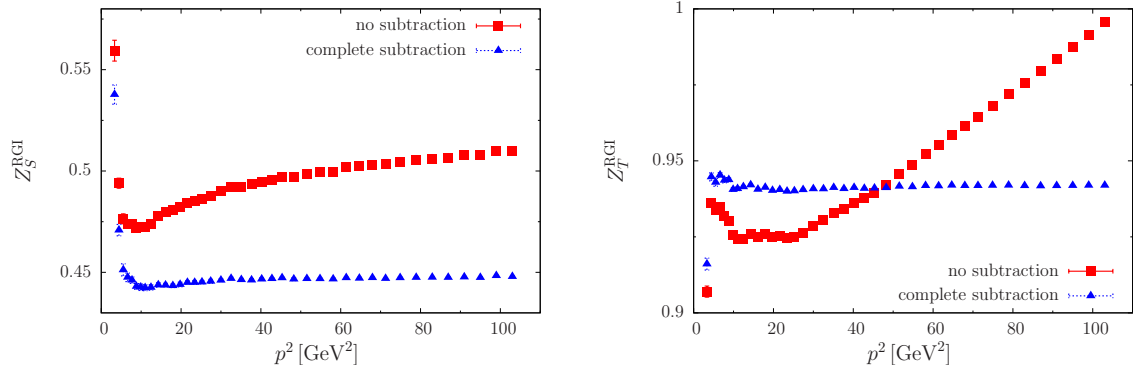
Figure 1: Z_S^{RGI} (left) and Z_T^{RGI} (right) for $\beta = 5.40$. The Z factors obtained without subtraction are shown as red squares, those with complete one-loop subtraction (14) as blue triangles. (The necessary scale transformation factors for the momenta are given at the end of Section 4.)

alternative method. One possibility which will be discussed in the next sections is a 'reduced' subtraction: Instead of subtracting the complete one-loop lattice artifacts we subtract only the one-loop terms proportional to a^2, if they are known for the given action.

4   Subtraction of order a^2 one-loop lattice artifacts

4.1   Lattice perturbation theory up to order $g^2 a^2$

The diagrammatic approach to compute the one-loop a^2 terms for the Z factors of local and one-link operators has been developed by some of us [6, 10]. The general case of Wilson type improved fermions is discussed in [11]. For details of the computations we refer to these references. Here we give explicitly the results for the operators and actions investigated in this paper (massless improved Wilson fermions with $c_{SW} = 1$, plaquette gauge action, Landau gauge).

Using the relation (6) we compute a common Z factor for each multiplet given in Table 1. The results are as follows:

$$
\begin{aligned}
Z_S &= 1 + \frac{g^2\,C_F}{16\pi^2}\left\{ -23.3099 + 3\,\log(a^2 S_2)\right.\\
&\quad +a^2\left[S_2\left(1.64089 - \frac{239}{240}\log(a^2 S_2)\right) + \frac{S_4}{S_2}\left(1.95104 - \frac{101}{120}\log(a^2 S_2)\right)\right]\left.\right\},\\
Z_V &= 1 + \frac{g^2\,C_F}{16\pi^2}\left\{ -15.3291\right.\\
&\quad +a^2\left[S_2\left(-1.33855 + \frac{151}{240}\log(a^2 S_2)\right) + \frac{S_4}{S_2}\left(2.89896 - \frac{101}{120}\log(a^2 S_2)\right)\right]\left.\right\},
\end{aligned}
$$

6

$$Z_A = 1 + \frac{g^2\,C_F}{16\pi^2}\left\{-13.7927 \right.$$
$$\left. +a^2\left[S_2\left(-0.92273 + \frac{151}{240}\log(a^2 S_2)\right) + \frac{S_4}{S_2}\left(2.89896 - \frac{101}{120}\log(a^2 S_2)\right)\right]\right\},$$

$$Z_T = 1 + \frac{g^2\,C_F}{16\pi^2}\left\{-11.1325 - \log(a^2 S_2) \right. \tag{17}$$
$$\left. +a^2\left[S_2\left(-1.72760 + \frac{221}{240}\log(a^2 S_2)\right) + \frac{S_4}{S_2}\left(3.21493 - \frac{101}{120}\log(a^2 S_2)\right)\right]\right\},$$

$$Z_{v_{2,a}} = 1 + \frac{g^2\,C_F}{16\pi^2}\left\{6.93831 - \frac{8}{3}\log(a^2 S_2) - \frac{2}{9}\frac{S_4}{(S_2)^2} \right.$$
$$+a^2\left[S_2\left(-1.50680 + \frac{167}{180}\log(a^2 S_2)\right)\right.$$
$$\left.\left. +\frac{S_4}{S_2}\left(2.63125 - \frac{197}{180}\log(a^2 S_2)\right) - \frac{71}{540}\frac{S_4{}^2}{(S_2)^3} - \frac{82}{135}\frac{S_6}{(S_2)^2}\right]\right\},$$

$$Z_{v_{2,b}} = 1 + \frac{g^2\,C_F}{16\pi^2}\left\{5.78101 - \frac{8}{3}\log(a^2 S_2) + \frac{4}{9}\frac{S_4}{(S_2)^2} \right.$$
$$+a^2\left[S_2\left(-0.56888 + \frac{1}{30}\log(a^2 S_2)\right)\right.$$
$$\left.\left. +\frac{S_4}{S_2}\left(-0.51323 + \frac{19}{30}\log(a^2 S_2)\right) + \frac{71}{270}\frac{S_4{}^2}{(S_2)^3} + \frac{164}{135}\frac{S_6}{(S_2)^2}\right]\right\}.$$

Here we have introduced the notation

$$S_n = \sum_{\lambda=1}^{4} p_\lambda^n\,, \tag{18}$$

with p_λ being the momentum components. Note that terms of type $(S_4/S_2)\log(a^2 S_2)$, appearing in Z_S, Z_V, Z_A, Z_T, all have the same coefficient which arises solely from the quark wave function renormalization constant Z_q. The corresponding one-loop vertex functions $\Gamma_i(p)$ in (6) do not contain such a structure. For later purposes we write the Z factors generically as

$$Z = 1 + \frac{g^2\,C_F}{16\pi^2}\,Z_{1-\text{loop}} + a^2\,g^2\,Z^{(a^2)}_{1-\text{loop}}(p,a)\,. \tag{19}$$

We emphasize that the numerical coefficients in the above expressions are either exact rationals or can be computed to a very high precision.

In Figs. 2, 3 and 4 we present $a^2\,g^2\,Z^{(a^2)}_{1-\text{loop}}(p,a)$ for selected operators as a function of $a^2 p^2$ on a finite lattice, where we choose the lattice momenta as $p_\lambda = (2\pi\,i_\lambda)/(a\,L_\lambda)$. Here, i_λ are integers and L_λ is the lattice extension in direction λ. We compare the correction terms for a general set of momenta with those obtained for the momenta used in this investigation at $\beta = 5.40$ on $24^3 \times 48$ lattices and with 'diagonal' momenta, i.e., momenta on the diagonal of the Brillouin zone.
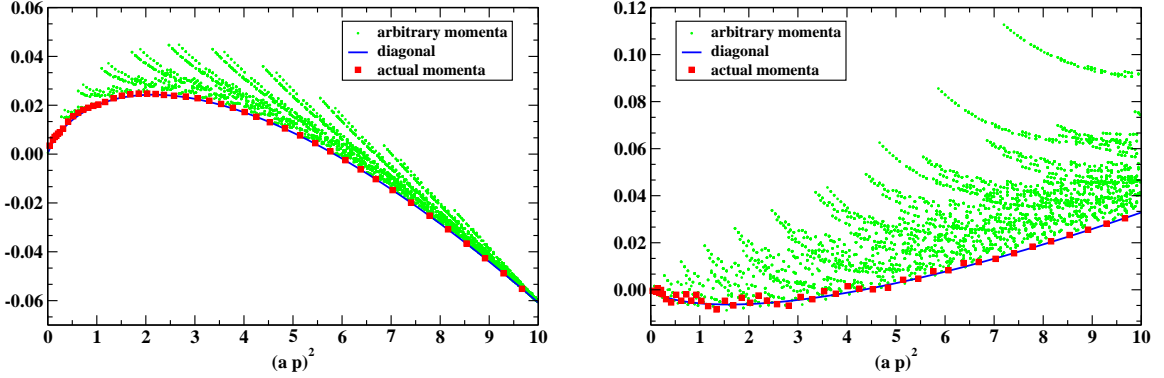
7

Figure 2: $a^2 g^2 Z_{1-\text{loop}}^{(a^2)}(p, a)$ for operators $\mathcal{O}^S$ (left) and $\mathcal{O}^V$ (right) as a function of $a^2 p^2$ on a $24^3 \times 48$ lattice at $\beta = 5.40$. The green filled circles are the values for an arbitrary set of (mostly non-diagonal) momenta, whereas the red filled squares are obtained from the momenta used in this investigation. The blue line is computed from diagonal momenta.
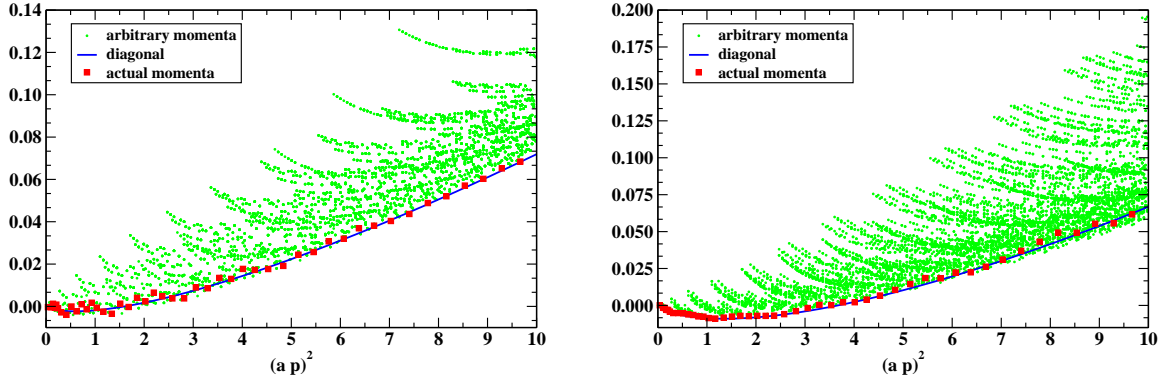

Figure 3: The same as Fig. 2 but for operators $\mathcal{O}^A$ (left) and $\mathcal{O}^T$ (right).
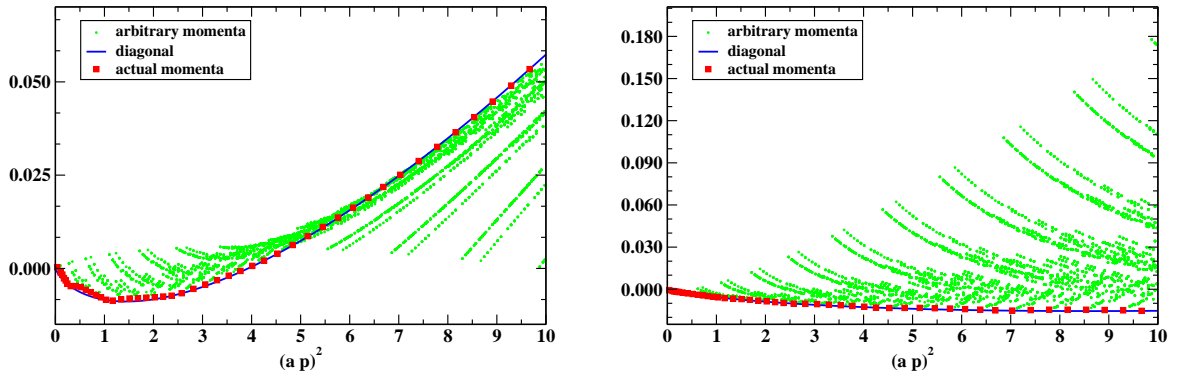
Figure 4: The same as Fig. 2 but for operators $\mathcal{O}^{v_2,a}$ (left) and $\mathcal{O}^{v_2,b}$ (right).

The figures show that the momenta of the actually measured Z factors are very close to the diagonal. Furthermore, one recognizes that the magnitude of the calculated one-loop a^2 corrections in the used momentum range is small but not negligible compared to the measured values which are of order 1 (see also Fig. 1). Therefore, one can expect that the subtraction of those terms yields a noticeable effect.

4.2 Subtraction of lattice artifacts up to order a^2

The subtraction procedure of order a^2 terms is not unique - we can use different definitions. The only restriction is that at one-loop order they should agree (treating $Z_{\mathrm{bare}}^{\mathrm{RI'-MOM}}(p,a)_{\mathrm{MC}}$ in perturbation theory). We investigate the following possibilities,

$$Z_{\mathrm{bare}}^{\mathrm{RI'-MOM}}(p,a)_{\mathrm{MC,sub,s}} = Z_{\mathrm{bare}}^{\mathrm{RI'-MOM}}(p,a)_{\mathrm{MC}} - a^2\,g_\star^2\,Z_{1-\mathrm{loop}}^{(a^2)}(p,a)\,, \tag{20}$$

$$Z_{\mathrm{bare}}^{\mathrm{RI'-MOM}}(p,a)_{\mathrm{MC,sub,m}} = Z_{\mathrm{bare}}^{\mathrm{RI'-MOM}}(p,a)_{\mathrm{MC}} \times \left(1 - a^2\,g_\star^2\,Z_{1-\mathrm{loop}}^{(a^2)}(p,a)\right)\,, \tag{21}$$

where $g_\star$ can be chosen to be either the bare lattice coupling g or the boosted coupling g_{B} (15). (In the following we denote subtraction type (20) by (s) and (21) by (m)). With ansatz (s) the one-loop a^2 correction is subtracted 'directly' from $Z_{\mathrm{bare}}^{\mathrm{RI'-MOM}}(p,a)_{\mathrm{MC}}$. Subtraction type (m) factorizes the one-loop a^2 correction from the nonperturbative Z factor.

The Z^{RGI} are computed from (10) using (s) or (m), where we expect slightly different numbers depending on the choice of coupling $g_\star$. The only significant errors to $Z_{\mathrm{bare}}^{\mathrm{RI'-MOM}}(p,a)_{\mathrm{MC,sub}}$ are due to the Monte Carlo simulations.

In Fig. 5 we show how the subtraction of lattice artifacts (complete and a^2) affects
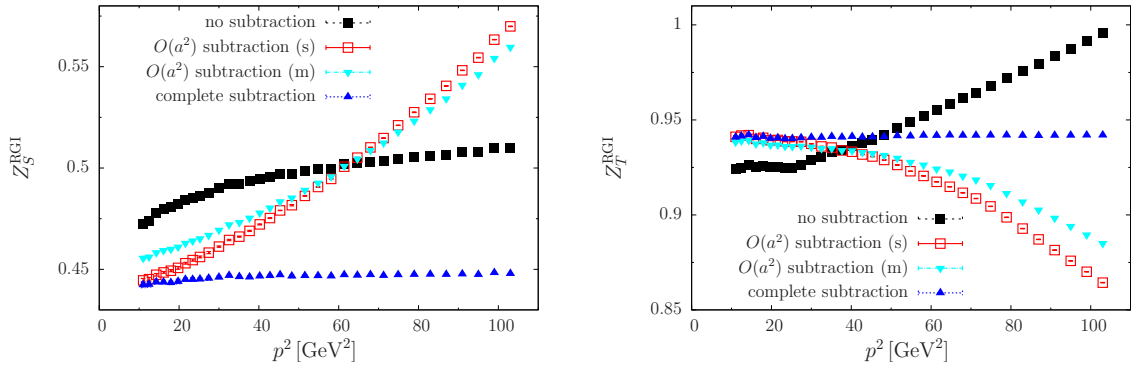

Figure 5: Unsubtracted and subtracted renormalization constants for the scalar operator $\mathcal{O}^S$ (left) and the tensor operator $\mathcal{O}^T$ (right) at $\beta = 5.40$, for $p^2 \gtrsim 10\,\mathrm{GeV}^2$ and $r_0\,\Lambda_{\overline{\mathrm{MS}}} = 0.700$. The complete subtraction is based on (14), whereas the a^2 subtractions are of type (s) and (m) with $g_\star = g_{\mathrm{B}}$.

the renormalization constants for the scalar and tensor operators. The complete one-loop subtraction results in a clear plateau for both Z^{RGI} factors. Using the a^2 subtractions there remains a more or less pronounced curvature which has to be fitted. From the definitions of the subtraction terms it is clear that they vanish at $a^2p^2 = 0$. Moreover, for

small $p^2 \approx 10\,\mathrm{GeV}^2$ the subtraction methods (**s**) and (14) already agree, as they should. However, as discussed above, Z^{RGI} can only be determined from sufficiently large momenta ($p^2 \gtrsim 10\,\mathrm{GeV}^2$), where differences arise between the various procedures. Therefore the results for Z^{RGI} may differ depending on the kind of subtraction. As can be seen in Fig. 5, this effect varies strongly from operator to operator.

4.3 Fit procedure

Compared to the complete one-loop subtraction we expect that $Z_{\mathrm{bare}}^{\mathrm{RI}'-\mathrm{MOM}}(p,a)_{\mathrm{MC,sub}}$ as computed from (**s**) or (**m**) contains terms proportional to a^{2n} ($n \geq 2$) even at order g^2, as well as the lattice artifacts from higher orders in perturbation theory, constrained only by hypercubic symmetry. Therefore, we parametrize the subtracted data for each β in terms of the hypercubic invariants S_n defined in (18) as follows

$$Z_{\mathrm{RI}'-\mathrm{MOM}}^{\mathcal{S}}(p)\, Z_{\mathrm{bare}}^{\mathrm{RI}'-\mathrm{MOM}}(p,a)_{\mathrm{MC,sub}} = \frac{Z^{\mathrm{RGI}}(a)}{\Delta Z^{\mathcal{S}}(p)\,\left[1 + b_1\,(g^{\mathcal{S}})^8\right]} + \tag{22}$$

$$a^2\left(c_1\,S_2 + c_2\,\frac{S_4}{S_2} + c_3\,\frac{S_6}{(S_2)^2}\right) + a^4\left(c_4\,(S_2)^2 + c_5\,S_4\right) + a^6\left(c_6\,(S_2)^3 + c_7\,S_4\,S_2 + c_8\,S_6\right)\ .$$

There are also further non-polynomial invariants at order a^4, a^6, but their behavior is expected to be well described by the invariants which have been included already. Ansatz (22) is a generalization of (16): After the 'reduced' one-loop subtraction of lattice artifacts the Z factors are expected to depend more strongly on a^4 or a^6 hypercubic invariants than after the complete one-loop subtraction (see Fig. 5). The parameters $c_1, \ldots, c_8$ describe the lattice artifacts.

Together with the target parameter $Z^{\mathrm{RGI}}(a)$ we have ten parameters for this general case. In view of the limited number of data points for each single β value (5.20, 5.25, 5.29, 5.40) we apply the ansatz (22) to several β values simultaneously with

$$\frac{Z^{\mathrm{RGI}}(a)}{\Delta Z^{\mathcal{S}}(p)\,\left[1 + b_1\,(g^{\mathcal{S}})^8\right]} \rightarrow \frac{Z^{\mathrm{RGI}}(a_k)}{\Delta Z_k^{\mathcal{S}}(p)\,\left[1 + b_1\,(g^{\mathcal{S}})^8\right]}\,, \tag{23}$$

where k labels the corresponding β value ($a_k = a(\beta_k)$). The parameters c_i are taken to be independent of β. This enhances the ratio (number of data points)/(number of fit parameters) significantly and we obtain several $Z^{\mathrm{RGI}}(a_k)$ at once. The fit is performed by a nonlinear model fit which uses - depending on the actual convergence - either the Nelder-Mead or a differential evolution algorithm [12]. Additionally, we have checked some of the fit results using MINUIT [13].

The renormalization factors are influenced by the choice for $r_0\,\Lambda_{\overline{\mathrm{MS}}}$. This quantity enters $\Delta Z^{\mathcal{S}}(M)$ in (8) via the corresponding coupling $g^{\mathcal{S}}(M)$ (for details see [4]). We choose $r_0\,\Lambda_{\overline{\mathrm{MS}}} = 0.700$ [14]. In order to estimate the influence of the choice of $r_0\,\Lambda_{\overline{\mathrm{MS}}}$ we also use $r_0\,\Lambda_{\overline{\mathrm{MS}}} = 0.789$ calculated in [15]. The Sommer scale r_0 is chosen to be $r_0 = 0.501\,\mathrm{fm}$ and the relation between the lattice spacing a and the inverse lattice coupling β is given by $r_0/a = 6.050\,(\beta = 5.20), 6.603\,(\beta = 5.25), 7.004\,(\beta = 5.29)$ and $8.285\,(\beta = 5.40)$ [16].

5 Renormalization factors for local and one-link operators

The fit procedure as sketched above has quite a few degrees of freedom and it is essential to investigate their influence carefully. A criterion for the choice of the minimal value of p^2 is provided by the breakdown of perturbation theory at small momenta. The data suggest [4] that we are on the 'safe side' when choosing $p^2_{\min} = 10\,\text{GeV}^2$. As the upper end of the fit interval we take the maximal available momentum at given coupling β.

Other important factors are

- **Type of subtraction:** As discussed above the procedure of the one-loop subtraction is not unique. We choose different definitions (**s**) and (**m**) with either bare g or boosted coupling g_B.

- **Selection of hypercubic invariants:** For the quality of the fit it is essential how well we describe the lattice artifacts which remain after subtraction [17, 18]. This is connected to the question whether the a^2 subtraction has been sufficient to subtract (almost) all a^2 artifacts. Therefore, we perform fits with various combinations of structures with coefficients c_i in (22). One should mention that the concrete optimal (i.e. minimal) set of c_i depends strongly on the momenta of the available Monte Carlo data - nearly diagonal momenta require fewer structures to be fitted than far off-diagonal ones.

The analysis should provide an optimal restricted set of parameters which can be used as a guideline for other classes of operators. Nevertheless, one has to inspect every new case carefully.

The results for Z^{RGI} will depend on the above mentioned factors. As a detailed presentation for all operators and β-values would be too lengthy, we select some operators and/or β values and take the corresponding results as a kind of reference. All results presented in this section are computed for $r_0\,\Lambda_{\overline{\text{MS}}} = 0.700$. The choice $r_0\,\Lambda_{\overline{\text{MS}}} = 0.789$ leads to qualitatively similar results. The large number of parameters in ansatz (22) calls for a combined use of the data sets at $\beta = (5.20, 5.25, 5.29, 5.40)$ for our fit analysis as indicated in (23). With the choice $p^2_{\min} = 10\,\text{GeV}^2$ this results in 94 data points available for the corresponding fits. Additionally, we should note that the errors on our fit parameters are those obtained from the nonlinear model fit. They differ from the error calculation for the Z^{RGI} based on (16) and used in [4].

5.1 Dependence on the subtraction type

In Fig. 6 we present the Z^{RGI} for operators $\mathcal{O}^S$, $\mathcal{O}^V$, $\mathcal{O}^T$ and $\mathcal{O}^{v2,a}$ for the different subtraction types using the fit ansatz (22) with all $c_i \neq 0$, i.e., we include a^2, a^4 and a^6 terms. From the discussion in Section 4.2 we expect that the resulting differences vary from operator to operator (cf. Fig. 5).

From Fig. 6 we observe that the complete one-loop subtraction (**1**) and the subtraction (**2**) agree within 1 %. This is not unexpected because the subtraction schemes are similar
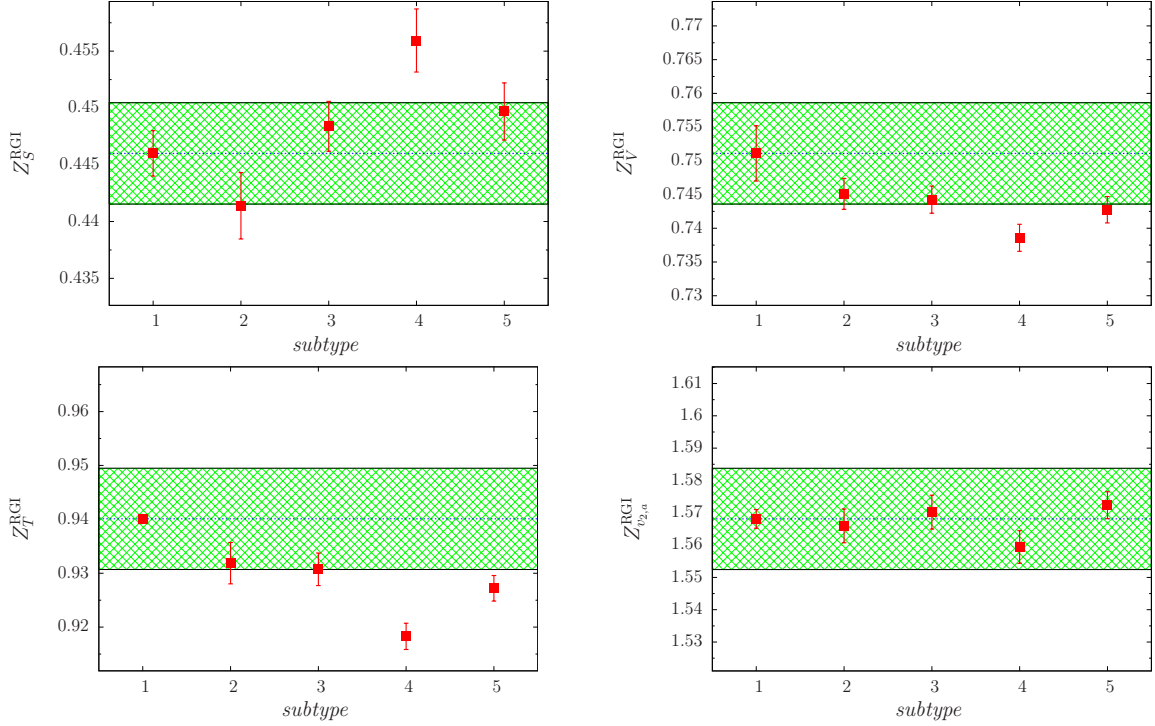
Figure 6: Z^{RGI} of selected operators at $\beta = 5.40$ as a function of the subtraction type (*subtype*): **1:** complete subtraction (14) with $g_\star = g_B$, **2:** (**s**) with $g_\star = g_B$, **3:** (**m**) with $g_\star = g_B$, **4:** (**s**) with $g_\star = g$, **5:** (**m**) with $g_\star = g$. The horizontal borders of the shaded area show a 1% deviation from case **1**.

and the gauge couplings coincide. The differences in the results for (**2**) and (**3**) can be used as an indication for a systematic uncertainty in the determination of Z^{RGI} based on the schemes (**s,m**). We observe that both subtraction approaches are numerically almost equivalent. Choices (**4**) and (**5**) lead to Z^{RGI} factors which are partly outside the 1% deviation. Generally, we recognize that all subtraction procedures for both bare and boosted couplings produce fit results within a reasonable error band width.

In order to test the effect of subtraction we compare the $g^2 a^2$ contributions as given in (17) with the remaining lattice artifacts of the Monte Carlo data fitted after subtraction, i.e. the result for (22) setting $Z^{\mathrm{RGI}}(a) = 0$. In Fig. 7 we show the results for the same selected operators choosing g_B. In the small p^2 region the remaining lattice artifacts are significantly smaller than the one-loop a^2 terms (operators $\mathcal{O}^S$, $\mathcal{O}^T$ and $\mathcal{O}^{v2,a}$). In case of already small one-loop a^2 artifacts (operator $\mathcal{O}^V$) the final artifacts remain small. This behavior strongly suggests to subtract the one-loop a^2 terms before applying the fit procedure.

Since the boosted coupling g_B is assumed to remove large lattice artifacts due to tadpole contributions in the perturbative series, we will use g_B in the following. In addition, we restrict ourselves to subtraction type (**s**), which is closest in spirit to the complete one-loop subtraction studied in [4] (leading approximately to a plateau in the Z^{RGI} as a function of p^2).

12
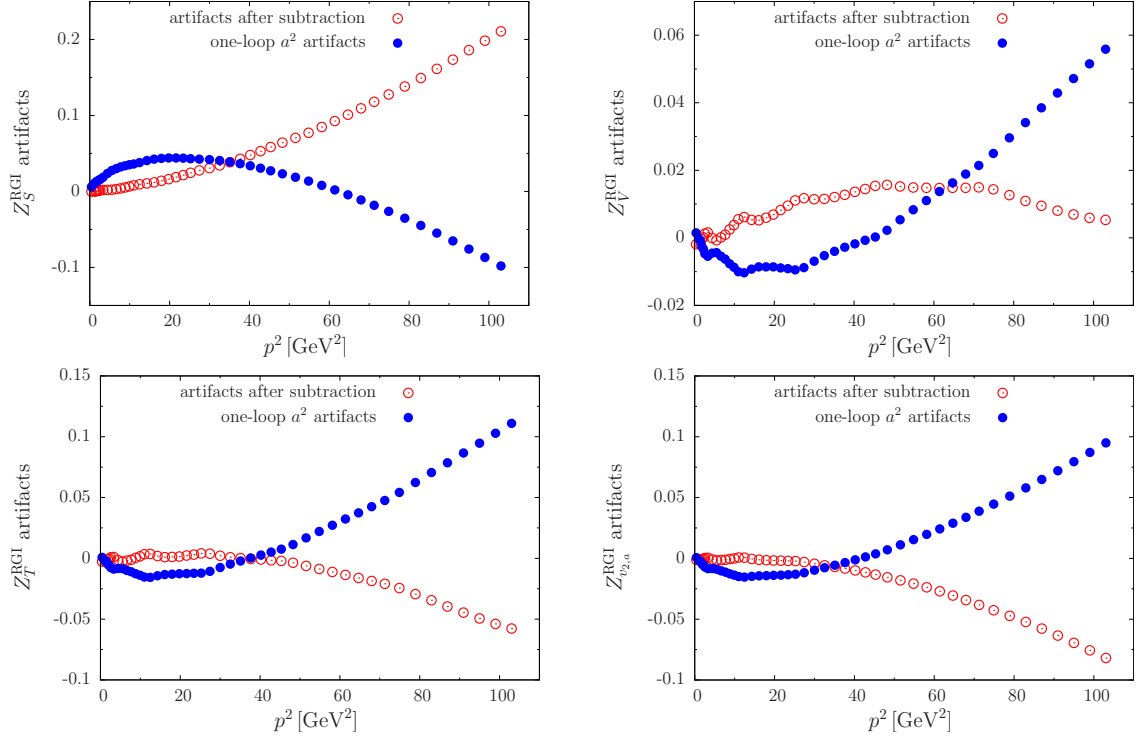
Figure 7: Lattice artifacts for Z^{RGI} of selected operators for $\beta = 5.40$ as a function of p^2 choosing $g_\star = g_B$. The blue filled circles are the corresponding $g^2 a^2$ correction terms, the red open circles are the fit results for (22) setting $Z^{\mathrm{RGI}}(a) = 0$.

5.2 Dependence on hypercubic invariants

Now we discuss the dependence on the hypercubic invariants included in the fit ansatz (22). The goal is to select a reasonable set of parameters to parametrize the remaining lattice artifacts. Figure 8 shows the fit results for some Z^{RGI} utilizing different parameter sets $\{c_k\}$. We use the subtraction type ($\mathbf{s}$) with $g_\star = g_B$. In that case the results from the complete one-loop subtraction ($\mathbf{1}$) serve as reference values.

Generally, we recognize that the resulting RGI renormalization factors do not vary significantly. Most fit results for Z^{RGI} are located in a $1\,\%$ deviation band around the corresponding complete subtraction results ($\mathbf{1}$). In addition, parametrizations ($\mathbf{2}$) and ($\mathbf{3}$) give almost identical fit results. This reflects, of course, the fact that our momenta are very close to the diagonal in the Brillouin zone. These restricted momentum sets might be the reason that even 'incomplete' hypercubic invariant sets ($\mathbf{4}$, $\mathbf{5}$) can be used to obtain reasonable fits. For the final results we use the fit with all $c_i \neq 0$ which would be natural in the case of more off-diagonal momenta.

In Figs. 9, 10 and 11 we show the results for all operators using the parameter sets with all c_i compared to the results obtained by the subtraction scheme based on (14).
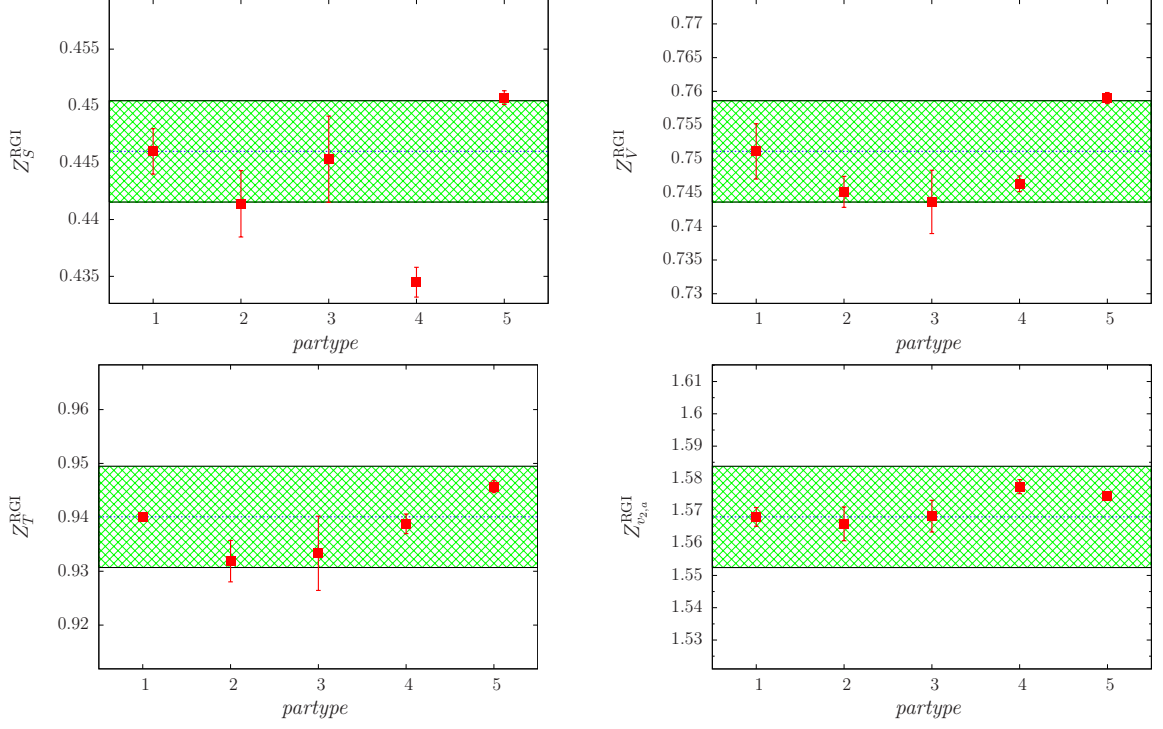
Figure 8: Z^{RGI} for selected operators at $\beta = 5.40$ as a function of the parameters included in the fit ansatz (22). The used parameter combinations (*partype*) are:
1: complete one-loop subtraction of lattice artifacts (14) **2:** all c_i, **3:** (c_1, c_4, c_6) - $O(4)$ invariant, **4:** $(c_1, c_2, c_3, c_4, c_5)$ - (a^2, a^4)- hypercubic invariants, **5:** $(c_4, c_5, c_6, c_7, c_8)$ - (a^4, a^6)- hypercubic invariants. The horizontal borders of the shaded area show a 1% deviation from case **1**.
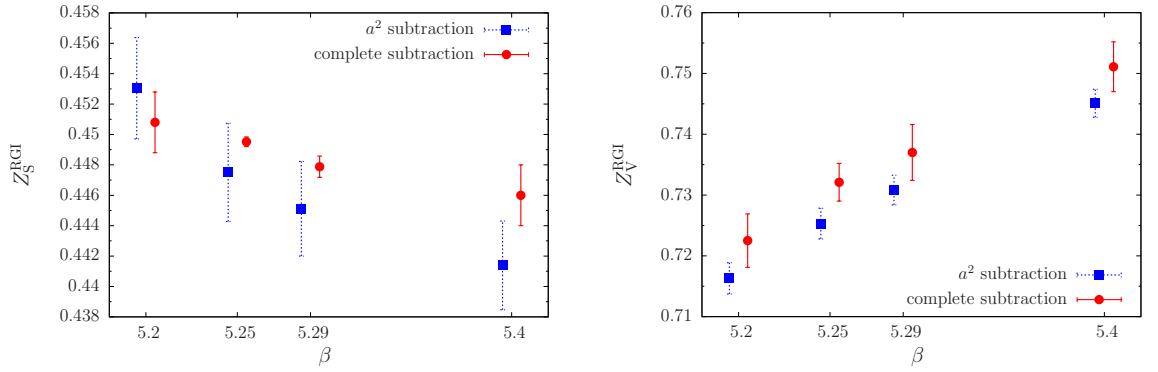
Figure 9: Z_S^{RGI} (left) and Z_V^{RGI} (right) at $r_0 \Lambda_{\overline{\mathrm{MS}}} = 0.700$ as a function of β using all c_i compared to the complete one-loop subtraction.
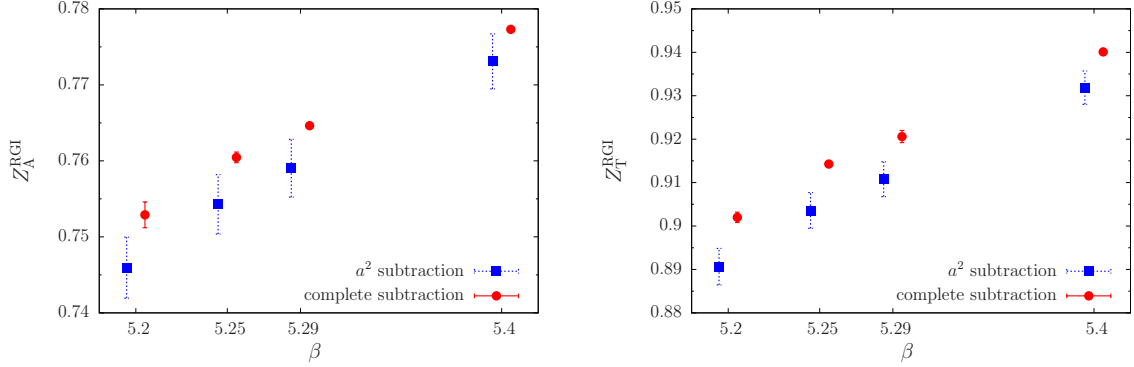
Figure 10: The same as in Fig. 9 for Z_A^{RGI} (left) and Z_T^{RGI} (right).
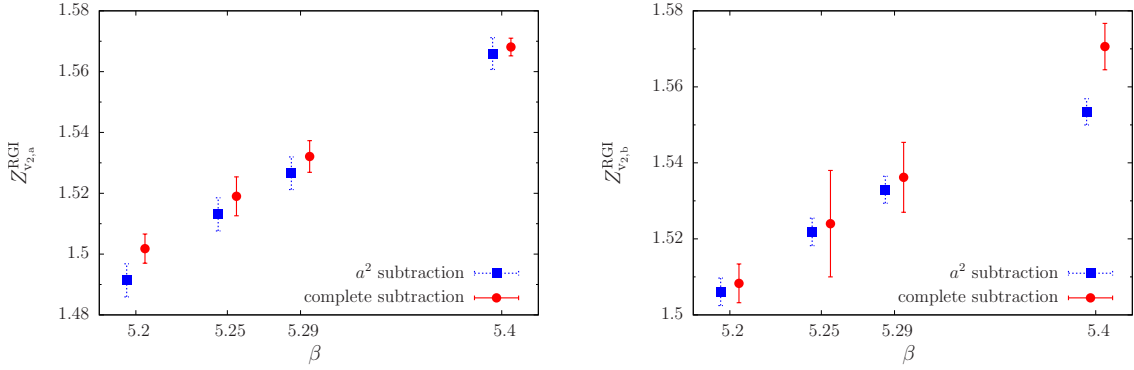
Figure 11: The same as in Fig. 9 for $Z_{v_{2,a}}^{\mathrm{RGI}}$ (left) and $Z_{v_{2,b}}^{\mathrm{RGI}}$ (right).

6 Results for local and one-link operators and conclusions

As a result of the preceding discussions we use subtraction type (**s**) (eq. (20)) with boosted coupling g_B and the fitting formula (22) with all c_i and b_1 coefficients to determine the Z^{RGI}. The final renormalization factors are collected in Table 2 using the two different $r_0 \Lambda_{\overline{\mathrm{MS}}}$ values 0.700 and 0.789. This shows the influence of the choice of $r_0 \Lambda_{\overline{\mathrm{MS}}}$ (depending on the anomalous dimension of the operator). For the investigated operators and β values we found for the relative differences of the Z^{RGI}

$$\delta Z^{\mathrm{RGI}} = \left| \frac{Z_{r_0\,\Lambda_{\overline{\mathrm{MS}}}=0.700}^{\mathrm{RGI}} - Z_{r_0\,\Lambda_{\overline{\mathrm{MS}}}=0.789}^{\mathrm{RGI}}}{Z_{r_0\,\Lambda_{\overline{\mathrm{MS}}}=0.700}^{\mathrm{RGI}}} \right| \lesssim 0.04 \,. \tag{24}$$

For comparison we collect in Table 3 the values for Z^{RGI} computed by means of fits with the ansatz (16) to data where a complete one-loop subtraction of lattice artifacts (according to (14) with $g_\star = g_{\mathrm{B}}$) has been performed. Note that here the errors are determined from the variation of the subtracted data between the scales $\mu^2 = 10, 20, 30 \, \mathrm{GeV}^2$ [4]. The reported renormalization factors are calculated for the values r_0/a given at the end of Section 4 and, therefore, differ from those given in [4]. The Z factors of the local operators

Op.	$r_0 \Lambda_{\overline{\mathrm{MS}}}$	$Z^{\mathrm{RGI}}|_{\beta=5.20}$	$Z^{\mathrm{RGI}}|_{\beta=5.25}$	$Z^{\mathrm{RGI}}|_{\beta=5.29}$	$Z^{\mathrm{RGI}}|_{\beta=5.40}$
$\mathcal{O}^S$	0.700	0.4530(34)	0.4475(33)	0.4451(32)	0.4414(30)
	0.789	0.4717(44)	0.4661(65)	0.4632(54)	0.4585(27)
$\mathcal{O}^V$	0.700	0.7163(26)	0.7253(26)	0.7308(25)	0.7451(24)
	0.789	0.7238(72)	0.7319(94)	0.7365(99)	0.7519(50)
$\mathcal{O}^A$	0.700	0.7460(41)	0.7543(40)	0.7590(39)	0.7731(37)
	0.789	0.7585(46)	0.7634(77)	0.7666(81)	0.7805(30)
$\mathcal{O}^T$	0.700	0.8906(43)	0.9036(42)	0.9108(41)	0.9319(39)
	0.789	0.8946(85)	0.9041(111)	0.9075(120)	0.9316(49)
$\mathcal{O}^{v2,a}$	0.700	1.4914(55)	1.5131(55)	1.5266(54)	1.5660(53)
	0.789	1.4635(108)	1.4776(112)	1.4926(90)	1.5397(58)
$\mathcal{O}^{v2,b}$	0.700	1.5061(37)	1.5218(37)	1.5329(36)	1.5534(35)
	0.789	1.4601(151)	1.4727(206)	1.4863(165)	1.5115(140)

Table 2: Z^{RGI} values using the subtraction (s) with g_B.

in both tables agree within 1 %. The Z factors of the one-link operators differ at most by 2 %.

Let us compare our results in Table 3 for the local vector current with Z_V^{RGI} obtained from an analysis of the proton electromagnetic form factor [19] following [20], which are listed in Table 4. The numbers agree within less than 1 % with the numbers in Table 3 ($r_0 \Lambda_{\overline{\mathrm{MS}}} = 0.700$), supporting the complete one-loop subtraction as our reference point.

From the present investigation we conclude: The alternatively proposed 'reduced' subtraction algorithm can be used for the determination of the renormalization factors if the complete subtraction method is not available. Possible applications could be Z factors for $N_f = 2+1$ calculations with more complicated fermionic and gauge actions where one-loop results to order a^2 are available (for the fermionic SLiNC action with improved Symanzik gauge action see Ref. [10]).

In this study we have analyzed data sets with momenta close to the diagonal of the Brillouin zone. The one-loop a^2 contributions to the Z factors are completely general and can be used for arbitrary (also non-diagonal) momentum sets. Our ansatz (22) allows to take into account the remaining artifacts after subtracting these one-loop a^2 terms. To get reasonable fit results the ratio (number of data points)/(number of fit parameters) has to be sufficiently large.

As we pointed out the subtraction type is not unique. With (s) and (m) we tested two different types. The resulting fits do not give a clear preference for one of these. Even

Op.	$r_0 \Lambda_{\overline{\mathrm{MS}}}$	$Z^{\mathrm{RGI}}|_{\beta=5.20}$	$Z^{\mathrm{RGI}}|_{\beta=5.25}$	$Z^{\mathrm{RGI}}|_{\beta=5.29}$	$Z^{\mathrm{RGI}}|_{\beta=5.40}$
$\mathcal{O}^S$	0.700	0.4508(20)	0.44952(32)	0.44788(70)	0.4460(20)
	0.789	0.4620(85)	0.4603(60)	0.4585(61)	0.4560(48)
$\mathcal{O}^V$	0.700	0.7225(44)	0.7321(31)	0.7370(46)	0.7511(41)
	0.789	0.7219(53)	0.7316(41)	0.7364(55)	0.7506(50)
$\mathcal{O}^A$	0.700	0.7529(17)	0.76046(70)	0.76463(33)	0.77731(20)
	0.789	0.7530(14)	0.76054(48)	0.7647(14)	0.7774(10)
$\mathcal{O}^T$	0.700	0.9020(12)	0.91427(24)	0.9206(14)	0.94009(69)
	0.789	0.8948(40)	0.9072(32)	0.9137(48)	0.9333(38)
$\mathcal{O}^{v2,a}$	0.700	1.5018(48)	1.5190(64)	1.5321(52)	1.5681(29)
	0.789	1.473(18)	1.490(14)	1.504(12)	1.540(14)
$\mathcal{O}^{v2,b}$	0.700	1.5083(51)	1.524(14)	1.5362(92)	1.5706(61)
	0.789	1.480(15)	1.497(28)	1.509(23)	1.5436(69)

Table 3: Z^{RGI} using a complete one-loop subtraction of lattice artifacts.

$Z^{\mathrm{RGI}}|_{\beta=5.20}$	$Z^{\mathrm{RGI}}|_{\beta=5.25}$	$Z^{\mathrm{RGI}}|_{\beta=5.29}$	$Z^{\mathrm{RGI}}|_{\beta=5.40}$
0.7296(4)	0.7355(3)	0.7401(2)	0.7521(3)

Table 4: Z^{RGI} values for operator V from the proton electromagnetic form factor analysis.

the additional choice for the coupling ($g_\star = g$ or $g_\star = g_B$) does not lead to significantly different results. Therefore, our final choice (**s**) (eq. (20) with $g_\star = g_B$) was supported by 'external' arguments: the improved behavior of the boosted perturbative series and the results obtained by complete one-loop subtraction [4].

We have shown that already the one-loop a^2 subtraction improves the behavior of the Z factors significantly: In the small p^2 region the contributions of the remaining lattice artifacts are smaller than the corresponding one-loop a^2 terms. As mentioned above, the accuracy to determine the Z factors is already at the 1 % level for local operators and at the 2 % level for operators with one covariant derivative compared to the complete one-loop subtraction of lattice artifacts. Additional systematic uncertainties are due to the choice of the $r_0 \Lambda_{\overline{\mathrm{MS}}}$ and r_0/a.

Appendix

In this Appendix we show that the definition (6) leads to renormalization factors which are invariant under the hypercubic group $H(4)$.

We consider a multiplet of local quark-antiquark operators $\mathcal{O}_i(x)$ ($i = 1, 2, \ldots, d$) in position space which transform according to

$$\mathcal{O}_i(x) \to S_{ij}(R)\, \mathcal{O}_j(R^{-1}x) \tag{A.1}$$

when

$$\psi(x) \to D(R)\, \psi(R^{-1}x) \,, \ \bar{\psi}(x) \to \bar{\psi}(R^{-1}x)\, D(R)^\dagger \tag{A.2}$$

for all $N = 384$ elements R of $H(4)$. Here $D(R)$ denotes the (unitary) spinor representation of $H(4)$ (or $O(4)$):

$$D(R)^\dagger \gamma_\mu D(R) = R_{\mu\nu}\gamma_\nu \,. \tag{A.3}$$

We assume that the operators $\mathcal{O}_i(x)$ have been chosen such that the $d \times d$-matrices $S(R)$ form a unitary irreducible representation of $H(4)$.

Denoting the unrenormalized vertex function at external momentum p of the operator $\mathcal{O}_i$ by $\Gamma_i(p)$ we have

$$\Gamma_i(p) = \sum_{j=1}^{d} S_{ij}(R)\, D(R)\, \Gamma_j(R^{-1}p)\, D(R)^\dagger \tag{A.4}$$

for all $R \in H(4)$, and analogously for the corresponding Born term $\Gamma_i^{\text{Born}}(p)$. Consequently we get

$$\sum_{i=1}^{d} \text{tr}\left[\Gamma_i(p)\Gamma_i(p)^\dagger\right] = \sum_{i=1}^{d} \text{tr}\left[\Gamma_i(Rp)\Gamma_i(Rp)^\dagger\right] \,. \tag{A.5}$$

Using the orthogonality relations for the matrix elements of irreducible representations one finds in addition

$$\sum_{R} \text{tr}\left[\Gamma_i(Rp)\Gamma_j(Rp)^\dagger\right] = \frac{1}{d}\delta_{ij}\sum_{k=1}^{d}\sum_{R} \text{tr}\left[\Gamma_k(Rp)\Gamma_k(Rp)^\dagger\right] \,, \tag{A.6}$$

where the sum extends over all $R \in H(4)$. The same relations hold when one of the vertex functions or both are replaced by the corresponding Born terms, e.g.,

$$\sum_{i=1}^{d} \text{tr}\left[\Gamma_i(p)\Gamma_i^{\text{Born}}(p)^\dagger\right] = \sum_{i=1}^{d} \text{tr}\left[\Gamma_i(Rp)\Gamma_i^{\text{Born}}(Rp)^\dagger\right] \,. \tag{A.7}$$

Therefore the renormalization condition

$$Z^{-1}Z_q = \frac{\sum_{i=1}^{d} \text{tr}\left[\Gamma_i(p)\,\Gamma_i^{\text{Born}}(p)^\dagger\right]}{\sum_{j=1}^{d} \text{tr}\left[\Gamma_j^{\text{Born}}(p)\,\Gamma_j^{\text{Born}}(p)^\dagger\right]} \tag{A.8}$$

or, equivalently,

$$Z^{-1} Z_q \delta_{ij} = \frac{d}{N} \frac{\sum_R \mathrm{tr} \left[\Gamma_i(Rp) \, \Gamma_j^{\mathrm{Born}}(Rp)^\dagger \right]}{\sum_{k=1}^d \mathrm{tr} \left[\Gamma_k^{\mathrm{Born}}(p) \, \Gamma_k^{\mathrm{Born}}(p)^\dagger \right]} \qquad (A.9)$$

respects the hypercubic symmetry, i.e., writing more precisely $Z = Z(p)$ we have $Z(Rp) = Z(p)$ for all $R \in H(4)$, and all lattice artefacts in Z must be invariant under the hypercubic group. Of course, here it has been assumed that $Z_q(Rp) = Z_q(p)$, as is the case for our definition (3) of Z_q.

Acknowledgements

References

[1] S. Capitani, Phys. Rept. **382** (2003) 113 [arXiv:hep-lat/0211036].

[2] G. Martinelli, C. Pittori, C. T. Sachrajda, M. Testa and A. Vladikas, Nucl. Phys. B **445** (1995) 81 [arXiv:hep-lat/9411010].

[3] R. Arthur and P. A. Boyle (RBC and UKQCD Collaborations), Phys. Rev. D **83** (2011) 114511 [arXiv:1006.0422[hep-lat]].

[4] M. Göckeler, R. Horsley, Y. Nakamura, H. Perlt, D. Pleiter, P. E. L. Rakow, A. Schäfer, G. Schierholz, A. Schiller, H. Stüben and J. M. Zanotti, (QCDSF/UKQCD Collaboration) Phys. Rev. D **82** (2010) 114511 [Erratum-ibid. D **86** (2012) 099903] [arXiv:1003.5756[hep-lat]].

[5] M. Göckeler, R. Horsley, E.-M. Ilgenfritz, H. Perlt, P. E. L. Rakow, G. Schierholz and A. Schiller, Phys. Rev. D **54** (1996) 5705 [arXiv:hep-lat/9602029].

[6] M. Constantinou, V. Lubicz, H. Panagopoulos and F. Stylianou, JHEP **0910** (2009) 064 [arXiv:0907.0381[hep-lat]].

[7] S. A. Larin, T. van Ritbergen and J. A. M. Vermaseren, Nucl. Phys. B **427** (1994) 41.

[8] A. Retey and J. A. M. Vermaseren, Nucl. Phys. B **604** (2001) 281 [arXiv:hep-ph/0007294].

[9] J. A. Gracey, JHEP **0610** (2006) 040 [arXiv:hep-ph/0609231].

[10] A. Skouroupathis and H. Panagopoulos, PoS LATTICE **2010**, 240 (2010).

[11] C. Alexandrou, M. Constantinou, T. Korzec, H. Panagopoulos and F. Stylianou, Phys. Rev. D **86** (2012) 014505 [arXiv:1201.5025[hep-lat]].

[12] Mathematica, Version 9.0, Wolfram Research, Inc., Champaign, IL (2012)

[13] MINUIT, Reference Manual, F. James, CERN Geneva, Switzerland (1994)

[14] QCDSF collaboration, in preparation.

[15] P. Fritzsch, F. Knechtli, B. Leder, M. Marinkovic, S. Schaefer, R. Sommer and F. Virotta (ALPHA Collaboration), Nucl. Phys. B **865** (2012) 397 [arXiv:1205.5380[hep-lat]].

[16] G. S. Bali, P. C. Bruns, S. Collins, M. Deka, B. Gläßle, M. Göckeler, L. Greil, T.R. Hemmert, R. Horsley, J. Najjar, Y. Nakamura, A. Nobile, D. Pleiter, P. E. L. Rakow, A. Schäfer, R. Schiel, G. Schierholz, A. Sternbeck and J. M. Zanotti (QCDSF Collaboration), Nucl. Phys. B **866** (2013) 1 [arXiv:1206.7034[hep-lat]].

[17] P. Boucaud, F. de Soto, J. P. Leroy, A. Le Yaouanc, J. Micheli, H. Moutarde, O. Pene and J. Rodriguez-Quintero, Phys. Lett. B **575** (2003) 256 [arXiv:hep-lat/0307026].

[18] F. de Soto and C. Roiesnel, JHEP **0709** (2007) 007 [arXiv:0705.3523[hep-lat]].

[19] S. Collins, M. Göckeler, P. Hägler, R. Horsley, Y. Nakamura, A. Nobile, D. Pleiter, P. E. L. Rakow, A. Schäfer, G. Schierholz, W. Schroers, H. Stüben, F. Winter and J. M. Zanotti (QCDSF/UKQCD Collaboration), Phys. Rev. D **84** (2011) 074507 [arXiv:1106.3580[hep-lat]].

[20] T. Bakeyev, M. Göckeler, R. Horsley, D. Pleiter, P. E. L. Rakow, G. Schierholz and H. Stüben (QCDSF/UKQCD Collaboration), Phys. Lett. B **580** (2004) 197 [arXiv:hep-lat/0305014].